

Published in final edited form as:

*Biomaterials*. 2013 January ; 34(2): 413–421. doi:10.1016/j.biomaterials.2012.09.052.

## The influence of hyaluronic acid hydrogel crosslinking density and macromolecular diffusivity on human MSC chondrogenesis and hypertrophy

Liming Bian<sup>a,b,1</sup>, Chieh Hou<sup>c,2</sup>, Elena Tous<sup>a,1</sup>, Reena Rai<sup>a,1</sup>, Robert L. Mauck<sup>a,c,2</sup>, and Jason A. Burdick<sup>a,c,\*</sup>

<sup>a</sup>Department of Bioengineering, University of Pennsylvania, Philadelphia, PA, USA

<sup>b</sup>Department of Mechanical and Automation Engineering, Biomedical Engineering Programme, the Chinese University of Hong Kong, Hong Kong

<sup>c</sup>McKay Orthopedic Research Laboratory, Department of Orthopedic Surgery, Perelman School of Medicine, University of Pennsylvania, Philadelphia, PA, USA

### Abstract

Hyaluronic acid (HA) hydrogels formed via photocrosslinking provide stable 3D hydrogel environments that support the chondrogenesis of mesenchymal stem cells (MSCs). Crosslinking density has a significant impact on the physical properties of hydrogels, including their mechanical stiffness and macromolecular diffusivity. Variations in the HA hydrogel crosslinking density can be obtained by either changes in the HA macromer concentration (1, 3, or 5% w/v at 15 min exposure) or the extent of reaction through light exposure time (5% w/v at 5, 10, or 15 min). In this work, increased crosslinking by either method resulted in an overall decrease in cartilage matrix content and more restricted matrix distribution. Increased crosslinking also promoted hypertrophic differentiation of the chondrogenically induced MSCs, resulting in more matrix calcification *in vitro*. For example, type X collagen expression in the high crosslinking density 5% 15 min group was ~156 and 285% higher when compared to the low crosslinking density 1% 15 min and 5% 5 min groups on day 42, respectively. Supplementation with inhibitors of the small GTPase pathway involved in cytoskeletal tension or myosin II had no effect on hypertrophic differentiation and matrix calcification, indicating that the differential response is unlikely to be related to force-sensing mechanotransduction mechanisms. When implanted subcutaneously in nude mice, higher crosslinking density again resulted in reduced cartilage matrix content, restricted matrix distribution, and increased matrix calcification. This study demonstrates that hydrogel properties mediated through alterations in crosslinking density must be considered in the context of the hypertrophic differentiation of chondrogenically induced MSCs.

### Keywords

Mesenchymal stem cells; Hyaluronic acid; Crosslinking; Chondrogenesis; Hypertrophy; Mineralization

---

© 2012 Elsevier Ltd. All rights reserved.

\*Corresponding author. University of Pennsylvania, Department of Bioengineering, 240 Skirkanich Hall, 210 S. 33rd Street, Philadelphia, PA 19104, USA. Tel.: +1 215 898 8537; fax: +1 215 573 2071. burdick2@seas.upenn.edu (J.A. Burdick).

<sup>1</sup>Tel.: +1 215 898 8537; fax: +1 215 573 2071.

<sup>2</sup>Tel.: +1 215 898 3294; fax: +1 215 573 2133.

## 1. Introduction

Mesenchymal stem cells (MSCs) are being explored as a clinically relevant cell source for regenerative medicine, especially for cartilage repair. These cells have been combined with a number of materials that support chondrogenic differentiation, including the natural polymer hyaluronic acid (HA) [1]. HA can be modified to support photocrosslinking into 3D hydrogels that support the chondrogenesis of MSCs [2]. The physical properties of hydrogels, including mechanical stiffness [3] and network porosity and permeability [4–6], have been shown to have a significant impact on the differentiation of encapsulated MSCs and localization of newly synthesized cartilage matrix [7,8]. Previously, we showed that changing the crosslinking density of HA hydrogels, by varying the HA macromer concentration alone, influences neocartilage formation and matrix distribution by encapsulated chondrocytes and bovine MSCs [8,9]. Alternatively, another way of modulating crosslinking density is by changing the ultraviolet light (UV) exposure time during gelation while keeping the HA macromer concentration constant. Importantly, this method decouples the effects of macromer concentration (i.e., HA content) from that of the crosslinking density. This is particularly important as HA is itself a biologic material, and cells, including human MSCs, possess CD44 and other receptors that interact with HA and initiate signaling cascades [10–12].

In addition to their ability to undergo chondrogenesis, MSCs also exhibit the tendency to undergo hypertrophic phenotype changes under chondrogenic induction, similar to that which is observed in the terminal differentiation of hypertrophic chondrocytes in the growth plate. This results in extensive calcification of the neocartilage matrix after ectopic transplantation in subcutaneous mouse models or with chemically defined hypertrophic challenge *in vitro* [13–15]. It is known that the components and structure of the extracellular and pericellular matrix play an important role in the regulation of chondrocyte hypertrophy and matrix calcification [16–18]. Chondrocytes entering terminal differentiation also substantially remodel their surrounding cartilage matrix to produce a template that facilitates mineralization [19]. Therefore, the physical properties of the hydrogel scaffold, such as crosslinking density, which control the quality and distribution of the newly formed cartilage matrix, may influence hypertrophic differentiation of the chondrogenically induced MSCs and consequently calcification of the neocartilage matrix. In addition, hypertrophic differentiation of chondrocytes is regulated by a plethora of large and small molecules, whose transport to encapsulated MSCs is regulated by the macromolecular diffusivity within and biochemical composition of the scaffold and newly formed cartilage matrix.

We previously showed that coculture of chondrocytes with MSCs, as well as mechanical loading influences hypertrophy [20,21]. Yet, there still exists the need to understand and better control mineralization towards the use of hydrogels as carriers for MSCs in cartilage repair. With these issues in mind, we hypothesize that the physical properties of hydrogels, which are dictated by the crosslinking density, will influence the initial chondrogenesis, neocartilage formation, and subsequent hypertrophy and matrix calcification by the encapsulated MSCs. Therefore, the objective of this study was to investigate the effect of variations in HA hydrogel crosslinking on the aforementioned processes in both *in vitro* and *in vivo* environments.

## 2. Material and methods

### 2.1. Macromer synthesis

Methacrylated HA (MeHA) was synthesized as previously reported [22]. Briefly, methacrylic anhydride (94%, FW: 154.17, Sigma) was added to a solution of 1 wt% HA (sodium hyaluronate powder, research grade, MW ~74 kDa, Lifecore) in deionized (DI)

water, adjusted to a pH of 8 with 5 N NaOH, and reacted on ice for 24 h. The macromer solution was purified via dialysis (MW cutoff 6–8 k) against deionized water for a minimum of 48 h with repeated changes of water. The final product was obtained by lyophilization and stored at  $-20^{\circ}\text{C}$  in powder form prior to use. The final macromer products were confirmed by  $^1\text{H}$  NMR to have a methacrylation level of  $\sim 29\%$ . Lyophilized macromers were dissolved in phosphate buffered saline (PBS) containing 0.05 wt% of the photoinitiator 2-methyl-1-[4-(hydroxyethoxy) phenyl]-2-methyl-1-propanone (I2959, Ciba) to allow for UV-mediated polymerization.

## 2.2. Sample preparation and in vitro culture

Human MSCs (Lonza) were expanded to passage 3 in growth media consisting of  $\alpha$ -MEM with 16.7% FBS and 1% pen/strep. MSCs (20 million/ml) were photo-encapsulated in 1, 3 or 5% w/v MeHA hydrogel disks with 15 min of UV exposure (wavelength: 360 nm; intensity:  $1.2\text{ mW/cm}^2$ ) or in 5% MeHA with 5, 10 or 15 min of UV exposure ( $\text{Ø} 5\text{ mm}$ , 2.6 mm thickness, Fig. 1A). Formed constructs were cultured in chondrogenic media (DMEM, 1% ITS + Premix, 50  $\mu\text{g/ml}$  L-proline, 0.1  $\mu\text{M}$  dexamethasone, 0.9 mM sodium pyruvate, 50  $\mu\text{g/ml}$  ascorbate, antibiotics) supplemented with transforming growth factor- $\beta 3$  (TGF- $\beta 3$ , 10 ng/ml), which was changed three times per week [23]. To induce hypertrophy, constructs were first cultured in chondrogenic media for 2 weeks. Media was then switched to hypertrophic induction media (1 nM dexamethasone, 1 nM triiodothyronine/T3 and 10 mM  $\beta$ -glycerophosphate/ $\beta$ -gly) from day 15 through day 42 of culture [24]. To decrease cytoskeletal tension, Y27632 (an inhibitor of the Rho-associated protein kinase/ROCK pathway) or blebbistatin (an inhibitor of non-muscle myosin II activity) was added to the hypertrophy induction media starting on day 15 at a concentration of 10 or 50  $\mu\text{M}$ , respectively (Fig. 1C) [25], and analyzed on day 28.

## 2.3. Characterization of HA hydrogels

The Young's moduli of acellular HA hydrogels were evaluated under unconfined compression with a dynamic mechanical analyzer (DMA, Q800 TA Instruments) at a strain rate of 10%/min, and moduli were calculated at a strain from 10 to 20%. The effective diffusivity of macromolecules in acellular HA hydrogels was determined by adapting a method described in a previous study [26]. Briefly, HA hydrogel disks were incubated in a fluorescein labeled dextran solution (10 kDa, 10  $\mu\text{g/ml}$ ; Molecular Probes) for 1, 2, 5 or 24 h. At each time point, a central slice of the hydrogel disk (0.39 mm thickness, spanning the full diameter) was removed and imaged to map the distribution of fluorescent intensity across the cross section. The average fluorescence intensity at each time point and location ( $n = 3$ ) was fit to a finite element simulation of diffusion. Briefly, finite element analysis was implemented using the FEBio open-resource finite element code (FEBio, <http://mrl.sci.utah.edu/software/febio>) to simulate dextran diffusion in a 3D finite element model of a quarter disk of the same size as our experimental samples [27]. Since randomly selected samples ( $n = 3$ ) were sacrificed and measured at each time point to obtain the average fluorescence intensity, a single estimated value of the effective diffusivity was derived by fitting the simulation curve to the experimental findings using the least squares method. The permeability of cell-seeded HA hydrogels was determined from confined compression testing. Briefly, MeHA disks were tested in confined compression in a PBS bath. After 300 s of tare loading, a 10% compressive strain (0.05%/s) was applied and samples were allowed to reach equilibrium (1200 s). Data from the stress relaxation test was extracted and fit to the Biphase Theory of Mow and co-workers to determine construct permeability ( $k$ ) and aggregate modulus ( $H_a$ ) [28]. The mesh sizes of the MeHA hydrogels were calculated based on the Flory–Rehner model and as previously reported [29–31].

## 2.4. Subcutaneous implantation in nude mice

MSC-laden (20 million/ml) HA hydrogel constructs of varying crosslinking density ( $n = 8$  for each group) were fabricated as described above and cultured in chondrogenic media for 2 weeks before being implanted (Fig. 1C). Four subcutaneous pockets were prepared on the backs of male nude mice (NCRNU, age 4 weeks; Taconic) and received implants. 8 samples of each hydrogel formulation were implanted into two mice. A total of ten mice were used to accommodate the five hydrogel formulations. Samples were harvested 4 weeks later for analysis. Guidelines from the Institutional Animal Care and Use Committee at the University of Pennsylvania were followed during all animal procedures.

## 2.5. Gene expression analysis

For gene expression analysis, samples were homogenized in Trizol Reagent (Invitrogen) with a tissue grinder, RNA was extracted according to the manufacturer's instructions, and the RNA concentration was determined using an ND-1000 spectrophotometer (Nanodrop Technologies). One microgram of RNA from each sample was reverse transcribed into cDNA using reverse transcriptase (Superscript II, Invitrogen) and oligoDT (Invitrogen). Polymerase chain reaction (PCR) was performed on an Applied Biosystems 7300 Real-Time PCR system using Taqman primers and probes specific for GAPDH (housekeeping gene) and other genes of interest. Sequences of the primers and probes used are listed in Table 1. The relative gene expression was calculated using the  $\Delta\Delta C_T$  method, where fold difference was calculated using the expression  $2^{\Delta\Delta C_T}$ . Each sample was internally normalized to GAPDH and each group was normalized to the expression levels of MSCs at the time of encapsulation (i.e., after expansion and before differentiation). Relative expression levels greater than 1 represent up-regulation with culture, while relative expression levels less than 1 represent down-regulation of that gene compared to that of initially encapsulated MSCs.

## 2.6. Biochemical analysis

One-half of each construct was weighed wet, lyophilized, reweighed dry, and digested in 0.5 mg/ml Proteinase-K (Fisher Scientific) at 56 °C for 16 h. The Pico-Green assay (Invitrogen, Molecular Probes) was used to quantify the DNA content of the constructs with Lambda phage DNA (0–1 mg/ml) as a standard [32]. For each sample, both the mass of the entire gel and the half gel used for DNA assay were measured. The total amount of DNA per sample was calculated by scaling the amount of DNA detected in the half gel by a weight ratio (total weight/half weight). The GAG content was measured using the dimethylmethylene blue (DMMB, Sigma Chemicals) dye-binding assay with shark chondroitin sulfate (0–50 mg/ml) as a standard [33]. The overall collagen content was assessed by measuring the orthohydroxyproline (OHP) content via dimethylaminobenzaldehyde and chloramine T assay. Collagen content was calculated by assuming a 1:7.5 OHP-to-collagen mass ratio [34]. The collagen and GAG contents were normalized to the disk wet weight.

## 2.7. Histological analysis

The remaining halves of the constructs were fixed in 4% formalin for 24 h, embedded in paraffin, and processed using standard histological procedures. The histological sections (8  $\mu\text{m}$  thick) were stained for targets of interest using the Vectastain ABC kit and the DAB Substrate kit for peroxidase (Vector Labs). Briefly, sections were predigested in 0.5 mg/ml hyaluronidase for 30 min at 37 °C and incubated in 0.5 N acetic acid for 4 h at 4 °C to swell the samples prior to overnight incubation with primary antibodies at dilutions of 1:100, 1:200, and 1:3 for chondroitin sulfate (mouse monoclonal anti-chondroitin sulfate, Sigma), and type I (mouse monoclonal anti-collagen type I, Sigma) and type II collagen antibodies (mouse monoclonal anti-collagen type II, Developmental Studies Hybridoma Bank),

respectively. Non-immune controls underwent the same procedure without primary antibody incubation.

## 2.8. Statistical analysis

All data are presented as mean  $\pm$  standard deviation. Statistica (Statsoft, Tulsa, OK) was used to perform statistical analyses using two-way ANOVA, followed by Tukey's HSD post hoc testing to allow comparison between groups ( $n = 4$  samples per group), with culture duration and experimental group as independent factors.

## 3. Results

### 3.1. Physical properties of HA hydrogels

HA hydrogels were formed by photopolymerization of MeHA solutions that had ~29% methacrylate modification. The cross-linking density of the HA hydrogels was increased by increasing the macromer concentration (1, 3, or 5% w/v) with a constant 15 min of UV exposure time or by photocrosslinking a 5% MeHA solution with increasing duration of UV exposure (5, 10 or 15 min) (Fig. 1A). In terms of bulk mechanical properties, the Young's modulus of the acellular hydrogels increased with increasing crosslinking density using both approaches (1% 15 min:  $3.5 \pm 0.2$  kPa; 3% 15 min:  $22.0 \pm 3.1$  kPa; 5% 15 min:  $53.6 \pm 4.5$  kPa; 5% 5 min:  $3.6 \pm 1.0$  kPa; 5% 10 min:  $24.1 \pm 5.8$  kPa; mean  $\pm$  standard deviation; Fig. 1B). Meanwhile, the effective diffusivity of fluorescently labeled dextran (MW: 10 kDa) in MeHA hydrogels decreased with increasing crosslinking density (Fig. 1B). Acellular 5% 5 min hydrogels swelled by ~40% and 1% 15 min hydrogels contracted by ~6% after 24 h of incubation in PBS (Fig. S1A). The mesh sizes of the 1% 15 min and 5% 5 min groups were calculated to be significantly higher than that of the 5% 15 min group (Fig. S1B).

MSC-seeded (20 million cells/ml) MeHA hydrogel constructs were also formed and cultured for 6 weeks *in vitro* with varying crosslink density (Fig. 1C). At early culture times (Day 1), a higher aggregate modulus and lower permeability were observed with higher crosslinking density, either by increasing macromer content or increasing UV exposure time (Fig. 2A and B). After 42 days of *in vitro* culture, a similar trend was still observed in the constructs fabricated with increasing UV exposure and constant macromer content (5% 5 min, 5% 10 min and 5% 15 min). However, constructs fabricated with lower HA content (1% 15 min and 3% 15 min) exhibited a significant increase in aggregate modulus and a decrease in permeability with respect to day 1, reaching similar values as found in constructs of higher HA content (5% 15 min) (Fig. 2A and B). Additionally, 1% 15 min constructs contracted by ~16% in volume over the culture period, while all other groups swelled significantly, with the largest swelling observed in the 5% 5 min constructs (an increase of ~73%) (Fig. 2C).

### 3.2. In vitro neocartilage formation and MSC hypertrophy

To evaluate the chondrogenic and hypertrophic differentiation of MSCs, real time polymerase chain reaction (qPCR) was performed for selected chondrogenic (type II collagen, aggrecan) and hypertrophic markers (type X collagen, matrix metalloproteinase 13/MMP13, and alkaline phosphatase/ALP). MSCs encapsulated in lower density HA hydrogels (1% 15 min) showed higher aggrecan expression compared to that of the higher macromer concentration hydrogels (5% 15 min) on day 28, whereas no statistically significant differences were detected in type II collagen expression among all the groups (Fig. 3). Increasing expression levels of type X collagen and ALP, major markers of hypertrophy, were observed with increasing crosslinking density introduced by either higher macromer concentration or longer UV exposure times (Fig. 3). For example, the type X collagen expression of the 5% 15 min group was ~156 and 285% higher compared to the 1% 15 min and 5% 5 min group on day 42, respectively. There was also an increasing trend of



MMP13 expression, another important hypertrophic marker, in constructs fabricated with constant HA content and increasing UV exposure time on day 28 (Fig. 3). Conversely, MMP13 expression was significantly higher in the low crosslinking density 1% 15 min group (the only group that showed contraction) compared to all other groups at the same time point (Fig. 3). Viability staining indicated that the majority (>90%) of encapsulated cells remained viable in all groups after 14 days of culture (Fig. S2).

After 42 days of *in vitro* culture, quantification of cartilage specific matrix components showed that MSC-seeded constructs with low crosslinking density (1% 15 min, 5% 5 min), fabricated using either a lower macromer concentration or shorter UV exposure time, possessed higher glycosaminoglycan (GAG) and collagen contents compared to constructs of high crosslinking density (for example, GAG content: 1% 15 min@ $0.85 \pm 0.10\%$  wet weight, 5% 5 min@ $0.45 \pm 0.02\%$  vs. 5% 15 min@ $0.26 \pm 0.02\%$ ) (Fig. 4A and B). The DNA contents of all groups were similar on day 42 (Fig. 4C). Immunohistochemistry staining against chondroitin sulfate and type II collagen showed that cartilage matrix in constructs with low crosslinking was more evenly distributed in the intercellular space, whereas cartilage matrix was mostly restricted to the pericellular area in constructs with high crosslinking density (Fig. 4D). Staining against type X collagen increased with increasing crosslinking density introduced by either higher macromer concentration or longer UV exposure times (Fig. S3). Interestingly, calcium content increased with increasing macromer content or UV exposure time in the MSC-seeded constructs on day 28 and 42 (Fig. 5A). The calcium content of the 5% 15 min group was ~116 and 96% higher compared to the 1% 15 min and 5% 5 min group on day 42, respectively. Von Kossa staining indicated increasing calcification mostly in the periphery of the constructs with increasing cross-linking density (Fig. 5B).

### 3.3. Inhibiting cytoskeletal tension

Inhibitors to Rho-associated protein kinase/ROCK (Y27632) and myosin II (blebbistatin) were supplemented to the media to probe the potential effect of cytoskeletal tension on the enhanced MSC hypertrophic differentiation in high crosslinking density hydrogels. Blebbistatin reduced the expression of hypertrophic markers including MMP13, type X collagen and alkaline phosphatase in high crosslinking density constructs (5% MeHA, 15 min UV exposure) whereas Y27632 had no effect (Fig. 6A). However, no statistically significant differences were found in the calcium content of the blebbistatin and Y27632 treated constructs compared to the control constructs, as indicated by calcium quantification and Von Kossa staining (Fig. 6B and C).

### 3.4. In vivo neocartilage formation

To evaluate the effect of hydrogel crosslinking under *in vivo* conditions, HA hydrogels were implanted in subcutaneous pockets of nude mice for 28 days after 14 days of *in vitro* culture. Implants of low crosslinking density (1% 15 min, 3% 15 min, 5% 5 min) were opaque and white and were palpably stiffer than implants of higher crosslinking density (5% 10 min, 5% 15 min), which were translucent and soft (Fig. 7D). All hydrogel groups were soft and translucent at the time of implantation (Fig. S4). These low crosslinking density constructs also had higher GAG and collagen contents but reduced calcium content compared to high crosslinking density constructs (Fig. 7A, B and C). Immunohistochemistry staining revealed similar trends of cartilage matrix localization as was observed *in vitro*. The low crosslinking density groups (1% 15 min, 5% 5 min) had intense and distributed staining for type II collagen and chondroitin sulfate (Fig. 7D). Conversely, the staining of these markers in high crosslink density groups was mostly localized to the pericellular region (Fig. 7D). Unlike *in vitro* results, Von Kossa staining indicated extensive calcification throughout the cross-sectional areas of the implanted constructs except for the 1% 15 min group, which displayed

more mineralization in the periphery compared to the interior region (Fig. 7D). Our previous work shows that acellular implants do not support the infiltration of cells, vascular structures, or matrix accumulation [14].

#### 4. Discussion

HA hydrogels are promising materials for application as cell carriers in the repair of cartilage defects. Recent *in vitro* studies demonstrated successful chondrogenesis of MSCs photo-encapsulated in HA hydrogels formed through the crosslinking of HA modified with methacrylate groups [2,8,35]. One important parameter in construct formation is the resultant crosslinking density, which has been shown to alter matrix elaboration and distribution [8,9]. In this study, using human MSCs, we demonstrated that the crosslinking density, controlled using two different approaches, dictates the physical properties of the HA hydrogel scaffold including mechanical stiffness, solute diffusivity and permeability. Consequently, this changing crosslink density had a substantial impact on initial chondrogenic events, neocartilage formation, and eventual hypertrophic differentiation and calcification by encapsulated human MSCs.

The crosslinking density was tuned by adjusting only one of the two parameters (i.e., HA macromer content or UV exposure time), while keeping the other constant during photocrosslinking. The range of HA macromer concentrations from 1% to 5% w/v was chosen to ensure stable hydrogel formation and viability of the encapsulated cells. Meanwhile, 15 min of UV exposure time was used to allow thorough reaction of the methacrylate groups as indicated by plateauing gel stiffness with prolonged exposure after 15 min (data not shown). At a high HA precursor concentration of 5%, a minimum of 5 min UV exposure time was required to form stable hydrogels. Therefore a 5% HA solution was exposed to 5, 10 or 15 min of UV exposure to achieve graded crosslinking density. Importantly, this method allows for the presentation of similar densities of HA chains, removing the biologic differences inherent to gels with different HA concentrations.

Low crosslinking density hydrogels fabricated with both methods (1% 15 min, 5% 5 min) not only favored the production of cartilage matrix, but also promoted its spatial distribution compared to the high crosslinking constructs. This was likely due to higher initial permeability in low crosslinking density hydrogels, which facilitates nutrient diffusion and distribution of newly synthesized cartilage matrix. However, there were some differences in the hydrogel structure created by these two methods. This was evidenced by the differential evolution of the two low cross-linking density groups, 1% 15 min and 5% 5 min, over 42 days of *in vitro* culture. These two groups developed higher cartilage matrix contents compared to the high crosslinking density groups, despite their initially more permeable network and therefore less capacity for retention of synthesized cartilage matrix molecules. However, constructs fabricated with 1% HA with 15 min of UV exposure were the only ones that experienced a volumetric contraction. It is known that MSCs exert a contractile traction force on the micro-environment under chondrogenic induction [36,37]. As a consequence, 1% HA hydrogels, which possessed low mechanical strength, decreased in size and resulted in a cell concentrating effect that promoted chondrogenesis [6,37]. On the other hand, even with a similarly low bulk stiffness as the 1% 15 min group, the significant swelling of 5% 5 min hydrogels indicated a different structure from that of the 1% HA hydrogels. The short UV exposure time allowed only partial consumption of the methacrylate groups, leaving some of methacrylates unreacted.

The quality of chondrogenic induction of MSCs and the resulting neocartilage matrix produced was closely associated with subsequent hypertrophic differentiation and matrix calcification. Previous studies showed that a hypertrophic cartilaginous template is required

for endochondral bone formation *in vivo* [15,38]. Gene expression profiling showed that MSCs encapsulated in high crosslinking density scaffolds expressed higher levels of hypertrophic markers, including type X collagen and alkaline phosphatase, resulting in more matrix calcification compared to MSCs in low crosslinking density scaffolds. One likely reason is that low crosslinking constructs contained higher levels of proteoglycans and type II collagen, both of which are known to promote chondrogenesis [39], inhibit hypertrophic differentiation [40] and matrix mineralization [18,41]. Furthermore, proteoglycans are also known to bind and stabilize various growth factors via the anionic domains, leading to enhanced bioactivity [42,43]. Some of the hypertrophy inhibitory growth factors such as TGF- $\beta$ s, either synthesized by the encapsulated cells or endogenously supplemented, were likely concentrated in the GAG rich low crosslinking density constructs than in the high crosslinking density ones. The higher overall content and more uniform spatial distribution of GAG in the low crosslinking density constructs possess a potentially larger capacity than high crosslinking density constructs to stabilize these anti-hypertrophy growth factors, which could become available to encapsulated MSCs. In addition, the higher initial permeability in low crosslinking density groups (1% 15 min, 5% 5 min) likely promoted diffusion of the hypertrophy inhibitory TGF- $\beta$ 3 into the hydrogels during the chondrogenic induction (the first two weeks of culture), resulting in reduced hypertrophic differentiation in these constructs.

Blebbistatin and Y27632 are known to lower the activity of myosin II and ROCK, respectively, which are involved in the generation of cell actomyosin tension. No obvious effect on MSC hypertrophy and matrix calcification was observed with the supplementation of these two inhibitors. Similar results were obtained when integrin binding RGD peptides were also incorporated into the HA hydrogels (data not shown). This indicates that the greater hypertrophic differentiation in the higher crosslinking density, and therefore stiffer, hydrogels was unlikely related to a mechanotransduction mechanism. In fact, RhoA/ROCK signaling, which is generally upregulated on stiff substrates, is known to suppress chondrocyte hypertrophy [44]. However, the influence of these factors on cells encapsulated with 3D hydrogels is less understood.

A surprising finding in this study was that the 1% 15 min group, which had a lower expression of hypertrophic markers including type X collagen and alkaline phosphatase and less calcification, expressed higher levels of MMP13, a hypertrophic marker, than higher crosslinking density groups (3% 15 min, 5% 15 min). It was noted that the 1% 15 min constructs were the only group that contracted during culture. Meanwhile, a previous study also reported that MMP13 expression by chondrocytes increased in contracting collagen gels, and that blocking contraction abolished this effect, suggesting a possible role of cell-matrix interactions [45]. Furthermore, the growth plate chondrocytes of MMP13-null mice undergo normal hypertrophy, but invasion of the ossification front is delayed, indicating that MMP13 facilitates the invasion of blood vessels and osteogenic cells but is not required for hypertrophic differentiation [46]. Therefore, under *in vitro* conditions the level of MMP13 was, to a lesser extent, related to the degree of hypertrophy. In addition, the capacity of MMP13 in promoting matrix calcification by degrading cartilaginous matrix and facilitating blood vessel ingression is likely limited in the covalently crosslinked MeHA hydrogels, which are generally impenetrable to blood vessel infiltration. This may explain the relatively low calcification in 1% 15 min implants *in vivo* despite the higher level of MMP13 expression compared to other groups.

MSC-seeded constructs were implanted in nude mice subcutaneously for an additional 4 weeks after 2 weeks of chondrogenic induction *in vitro* to evaluate neocartilage formation and hypertrophic calcification under *in vivo* conditions. Here, correlations between hydrogel crosslinking density and cartilage matrix production, distribution and calcification mirrored



that seen *in vitro*. Intriguingly, calcification was mostly localized in the peripheral region of the constructs during *in vitro* analysis, whereas it was much more extensive and distributed *in vivo*. The complex environment of *in vivo* implantation site involved several confounding factors such as vascularization, macrophages, fibrous capsule formation, all of which could have modulated the behavior of implanted MSCs.

Although the findings of this study are quite interesting towards the development of constructs for cartilage tissue engineering, there are several limitations to be noted. With regards to the diffusion study, a relatively small sized dextran (MW: 10 kDa) was used in experiments, which may not be representative of all molecules that may be present throughout the hydrogels. Another limitation of this study is that the *in vivo* neocartilage formation and hypertrophic calcification was evaluated in the subcutaneous space of the nude mice, which is only a preliminary assessment of the *in vivo* response of the hydrogel implants. It is recognized that a more clinically relevant *in vivo* location, such as in an articulating joint surface in large animals, will be needed to clearly assess chondrogenesis and hypertrophic calcification.

## 5. Conclusions

Our findings demonstrate that HA hydrogel crosslinking density regulates chondrogenesis, neocartilage matrix deposition, hypertrophic differentiation and matrix calcification by encapsulated human MSCs. Specifically, increased hydrogel crosslink density decreased cartilage matrix development and distribution, and promoted hypertrophic conversion and mineralization of encapsulated human MSCs, both *in vitro* and *in vivo*. Importantly, by varying the initial crosslink density, independent of HA macromer concentration, our approach decouples the biologic activity of HA from its role in hydrogel mechanics and diffusivity. Knowledge obtained from this study will be important in the design and optimization of hydrogels that maximize chondrogenesis and neocartilage development by encapsulated MSCs, while limiting their propensity to form mineralized constructs upon implantation. However, additional work is required to elucidate the precise mechanisms underlying the observed correlation between scaffold properties and hypertrophic differentiation.

## Supplementary Material

Refer to Web version on PubMed Central for supplementary material.

## Acknowledgments

This work was supported by National Institutes of Health grant R01EB008722. The authors thank Ms. Emily Zhang for her assistance in the experimental work.

## References

1. Huang AH, Farrell MJ, Mauck RL. Mechanics and mechanobiology of mesenchymal stem cell-based engineered cartilage. *J Biomech.* 2010; 43(1):128–36. [PubMed: 19828149]
2. Chung C, Beecham M, Mauck RL, Burdick JA. The influence of degradation characteristics of hyaluronic acid hydrogels on *in vitro* neocartilage formation by mesenchymal stem cells. *Biomaterials.* 2009; 30(26):4287–96. [PubMed: 19464053]
3. Engler AJ, Sen S, Sweeney HL, Discher DE. Matrix elasticity directs stem cell lineage specification. *Cell.* 2006; 126(4):677–89. [PubMed: 16923388]
4. Kempainen JM, Hollister SJ. Differential effects of designed scaffold permeability on chondrogenesis by chondrocytes and bone marrow stromal cells. *Biomaterials.* 2010; 31(2):279–87. [PubMed: 19818489]

5. Serpooshan V, Julien M, Nguyen O, Wang H, Li A, Muja N, et al. Reduced hydraulic permeability of three-dimensional collagen scaffolds attenuates gel contraction and promotes the growth and differentiation of mesenchymal stem cells. *Acta Biomater.* 2010; 6(10):3978–87. [PubMed: 20451675]
6. Vickers SM, Gotterbarm T, Spector M. Cross-linking affects cellular condensation and chondrogenesis in type II collagen-GAG scaffolds seeded with bone marrow-derived mesenchymal stem cells. *J Orthop Res.* 2010; 28(9):1184–92. [PubMed: 20225321]
7. Bryant SJ, Nuttelman CR, Anseth KS. The effects of crosslinking density on cartilage formation in photocrosslinkable hydrogels. *Biomed Sci Instrum.* 1999; 35:309–14. [PubMed: 11143369]
8. Erickson IE, Huang AH, Sengupta S, Kestle S, Burdick JA, Mauck RL. Macromer density influences mesenchymal stem cell chondrogenesis and maturation in photocrosslinked hyaluronic acid hydrogels. *Osteoarthr Cartil.* 2009; 17(12):1639–48. [PubMed: 19631307]
9. Chung C, Mesa J, Randolph MA, Yaremchuk M, Burdick JA. Influence of gel properties on neocartilage formation by auricular chondrocytes photo-encapsulated in hyaluronic acid networks. *J Biomed Mater Res A.* 2006; 77(3):518–25. [PubMed: 16482551]
10. Chen WY, Abatangelo G. Functions of hyaluronan in wound repair. *Wound Repair Regen.* 1999; 7(2):79–89. [PubMed: 10231509]
11. Lisignoli G, Cristino S, Piacentini A, Cavallo C, Caplan AI, Facchini A. Hyaluronan-based polymer scaffold modulates the expression of inflammatory and degradative factors in mesenchymal stem cells: involvement of Cd44 and Cd54. *J Cell Physiol.* 2006; 207(2):364–73. [PubMed: 16331675]
12. Zhu H, Mitsuhashi N, Klein A, Barsky LW, Weinberg K, Barr ML, et al. The role of the hyaluronan receptor CD44 in mesenchymal stem cell migration in the extracellular matrix. *Stem Cells.* 2006; 24(4):928–35. [PubMed: 16306150]
13. Pelttari K, Winter A, Steck E, Goetzke K, Hennig T, Ochs BG, et al. Premature induction of hypertrophy during in vitro chondrogenesis of human mesenchymal stem cells correlates with calcification and vascular invasion after ectopic transplantation in SCID mice. *Arthritis Rheum.* 2006; 54(10):3254–66. [PubMed: 17009260]
14. Bian L, Zhai DY, Tous E, Rai R, Mauck RL, Burdick JA. Enhanced MSC chondrogenesis following delivery of TGF-beta3 from alginate microspheres within hyaluronic acid hydrogels in vitro and in vivo. *Biomaterials.* 2011; 32(27):6425–34. [PubMed: 21652067]
15. Jukes JM, Both SK, Leusink A, Sterk LM, van Blitterswijk CA, de Boer J. Endochondral bone tissue engineering using embryonic stem cells. *Proc Natl Acad Sci U S A.* 2008; 105(19):6840–5. [PubMed: 18467492]
16. Boskey AL. The role of extracellular matrix components in dentin mineralization. *Crit Rev Oral Biol Med.* 1991; 2(3):369–87. [PubMed: 1654141]
17. Anderson HC. Molecular biology of matrix vesicles. *Clin Orthop Relat Res.* 1995; 314:266–80. [PubMed: 7634645]
18. Jubeck B, Gohr C, Fahey M, Muth E, Matthews M, Mattson E, et al. Promotion of articular cartilage matrix vesicle mineralization by type I collagen. *Arthritis Rheum.* 2008; 58(9):2809–17. [PubMed: 18759309]
19. Ortega N, Behonick DJ, Werb Z. Matrix remodeling during endochondral ossification. *Trends Cell Biol.* 2004; 14(2):86–93. [PubMed: 15102440]
20. Bian L, Zhai DY, Mauck RL, Burdick JA. Coculture of human mesenchymal stem cells and articular chondrocytes reduces hypertrophy and enhances functional properties of engineered cartilage. *Tissue Eng Part A.* 2011; 17(7–8):1137–45. [PubMed: 21142648]
21. Bian L, Zhai DY, Zhang EC, Mauck RL, Burdick JA. Dynamic compressive loading enhances cartilage matrix synthesis and distribution and suppresses hypertrophy in hMSC-laden hyaluronic acid hydrogels. *Tissue Eng Part A.* 2012; 18(7–8):715–24. [PubMed: 21988555]
22. Smeds KA, Pfister-Serres A, Miki D, Dastgheib K, Inoue M, Hatchell DL, et al. Photocrosslinkable polysaccharides for in situ hydrogel formation. *J Biomed Mater Res.* 2001; 54(1):115–21. [PubMed: 11077410]

23. Byers BA, Mauck RL, Chiang IE, Tuan RS. Transient exposure to transforming growth factor beta 3 under serum-free conditions enhances the biomechanical and biochemical maturation of tissue-engineered cartilage. *Tissue Eng Part A*. 2008; 14(11):1821–34. [PubMed: 1861145]
24. Mueller MB, Tuan RS. Functional characterization of hypertrophy in chondrogenesis of human mesenchymal stem cells. *Arthritis Rheum*. 2008; 58(5):1377–88. [PubMed: 18438858]
25. McBeath R, Pirone DM, Nelson CM, Bhadriraju K, Chen CS. Cell shape, cytoskeletal tension, and RhoA regulate stem cell lineage commitment. *Dev Cell*. 2004; 6(4):483–95. [PubMed: 15068789]
26. Albro MB, Li R, Banerjee RE, Hung CT, Ateshian GA. Validation of theoretical framework explaining active solute uptake in dynamically loaded porous media. *J Biomech*. 2010; 43(12):2267–73. [PubMed: 20553797]
27. Maas SA, Ellis BJ, Ateshian GA, Weiss JA. FEBio: finite elements for biomechanics. *J Biomech Eng*. 2012; 134(1):01100501–10.
28. Mow VC, Kuei SC, Lai WM, Armstrong CG. Biphasic creep and stress relaxation of articular cartilage in compression: theory and experiments. *J Biomech Eng*. 1980; 102:73–84. [PubMed: 7382457]
29. Baier Leach J, Bivens KA, Patrick CW Jr, Schmidt CE. Photocrosslinked hyaluronic acid hydrogels: natural, biodegradable tissue engineering scaffolds. *Biotechnol Bioeng*. 2003; 82(5):578–89. [PubMed: 12652481]
30. Metters AT, Anseth KS, Bowman CN. Fundamental studies of biodegradable hydrogels as cartilage replacement materials. *Biomed Sci Instrum*. 1999; 35:33–8. [PubMed: 11143373]
31. Flory, PJ. Principles of polymer chemistry. Ithaca: NY: Cornell University Press; 1953.
32. McGowan KB, Kurtis MS, Lottman LM, Watson D, Sah RL. Biochemical quantification of DNA in human articular and septal cartilage using PicoGreen and Hoechst 33258. *Osteoarthr Cartil*. 2002; 10(7):580–7. [PubMed: 12127839]
33. Farndale RW, Buttle DJ, Barrett AJ. Improved quantitation and discrimination of sulphated glycosaminoglycans by use of dimethylmethylene blue. *Biochim Biophys Acta*. 1986; 883(2):173–7. [PubMed: 3091074]
34. Hollander AP, Heathfield TF, Webber C, Iwata Y, Bourne R, Rorabeck C, et al. Increased damage to type II collagen in osteoarthritic articular cartilage detected by a new immunoassay. *J Clin Invest*. 1994; 93(4):1722–32. [PubMed: 7512992]
35. Chung C, Burdick JA. Influence of three-dimensional hyaluronic acid micro-environments on mesenchymal stem cell chondrogenesis. *Tissue Eng Part A*. 2009; 15(2):243–54. [PubMed: 19193129]
36. Li Q, Liu T, Zhang L, Liu Y, Zhang W, Liu W, et al. The role of bFGF in down-regulating alpha-SMA expression of chondrogenically induced BMSCs and preventing the shrinkage of BMSC engineered cartilage. *Biomaterials*. 2011; 32(21):4773–81. [PubMed: 21459437]
37. Vickers SM, Squitieri LS, Spector M. Effects of crosslinking type II collagen-GAG scaffolds on chondrogenesis in vitro: dynamic pore reduction promotes cartilage formation. *Tissue Eng*. 2006; 12(5):1345–55. [PubMed: 16771647]
38. Scotti C, Tonnarelli B, Papadimitropoulos A, Scherberich A, Schaeren S, Schauerte A, et al. Recapitulation of endochondral bone formation using human adult mesenchymal stem cells as a paradigm for developmental engineering. *Proc Natl Acad Sci U S A*. 2010; 107(16):7251–6. [PubMed: 20406908]
39. Bosnakovski D, Mizuno M, Kim G, Takagi S, Okumura M, Fujinaga T. Chondrogenic differentiation of bovine bone marrow mesenchymal stem cells (MSCs) in different hydrogels: influence of collagen type II extracellular matrix on MSC chondrogenesis. *Biotechnol Bioeng*. 2006; 93(6):1152–63. [PubMed: 16470881]
40. Varghese S, Hwang NS, Canver AC, Theprungsirikul P, Lin DW, Elisseeff J. Chondroitin sulfate based niches for chondrogenic differentiation of mesenchymal stem cells. *Matrix Biol*. 2008; 27(1):12–21. [PubMed: 17689060]
41. Chen CC, Boskey AL, Rosenberg LC. The inhibitory effect of cartilage proteoglycans on hydroxyapatite growth. *Calcif Tissue Int*. 1984; 36(3):285–90. [PubMed: 6205734]
42. Hubbell JA. Materials as morphogenetic guides in tissue engineering. *Curr Opin Biotechnol*. 2003; 14(5):551–8. [PubMed: 14580588]

43. Hynes RO. The extracellular matrix: not just pretty fibrils. *Science*. 2009; 326(5957):1216–9. [PubMed: 19965464]
44. Wang G, Woods A, Sabari S, Pagnotta L, Stanton LA, Beier F. RhoA/ROCK signaling suppresses hypertrophic chondrocyte differentiation. *J Biol Chem*. 2004; 279(13):13205–14. [PubMed: 14726536]
45. Berendsen AD, Vonk LA, Zandieh-Doulabi B, Everts V, Bank RA. Contraction-induced Mmp13 and –14 expression by goat articular chondrocytes in collagen type I but not type II gels. *J Tissue Eng Regen Med*. 2011 Epub ahead of print.
46. Stickens D, Behonick DJ, Ortega N, Heyer B, Hartenstein B, Yu Y, et al. Altered endochondral bone development in matrix metalloproteinase 13-deficient mice. *Development*. 2004; 131(23): 5883–95. [PubMed: 15539485]

## Appendix A. Supplementary data

Supplementary data related to this article can be found at <http://dx.doi.org/10.1016/j.biomaterials.2012.09.052>.

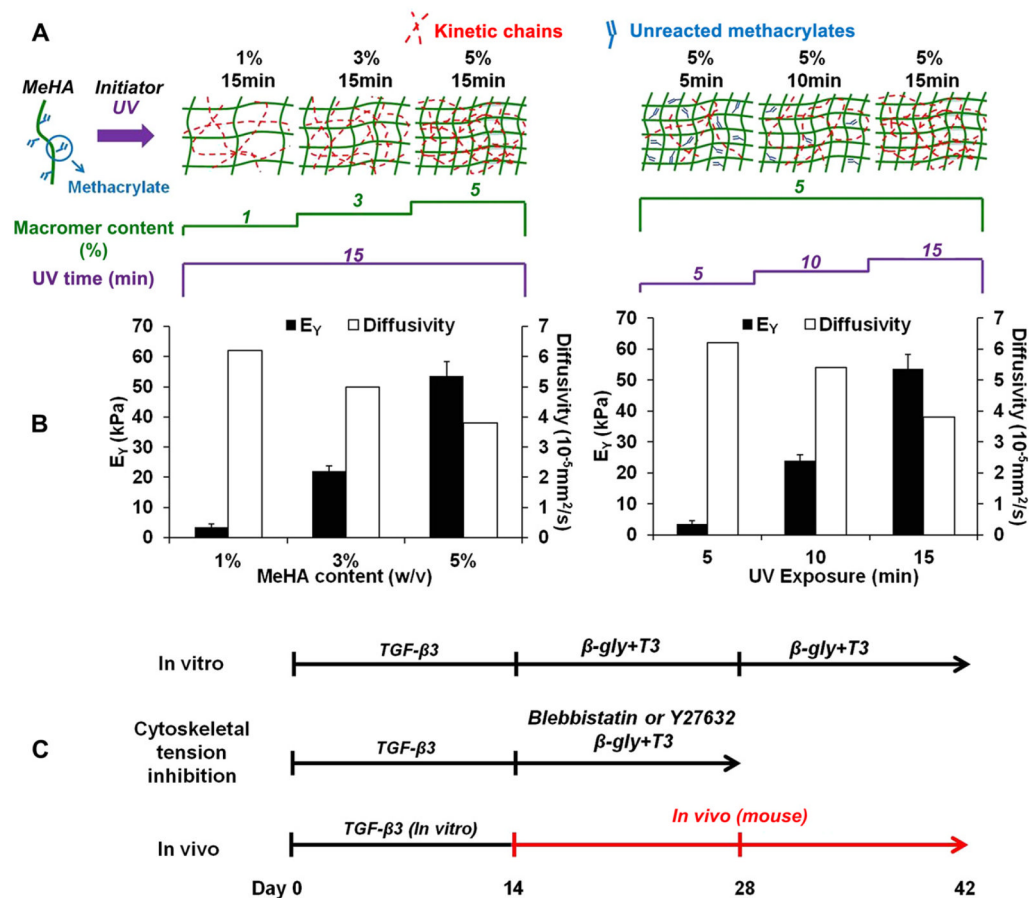


**Fig. 1.** Fabrication of methacrylated HA (MeHA) hydrogels with varying crosslinking density by changing either the macromer concentration or the exposure time (A); MeHA hydrogel Young's modulus and effective diffusivity of dextran (MW: 10 kDa) with varying crosslinking density (B); timeline and media supplements of the various studies to investigate crosslink density effects on cartilage formation and hypertrophy (C).



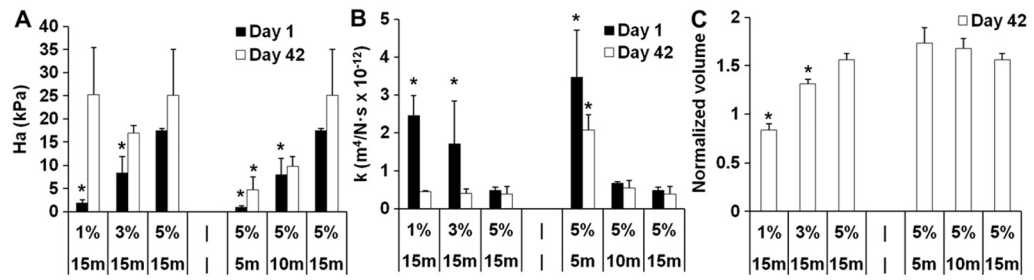


**Fig. 2.** Biphase parameters of aggregate modulus ( $H_a$ ) (A), permeability ( $k$ ) (B), and construct volume (normalized to the initial day 0 volume) (C) Of MSC-laden HA hydrogel constructs after 1 or 42 days of *in vitro* culture. \* $p < 0.05$  vs. 5% 15 min group at the same culture time; ( $n = 4$ ).

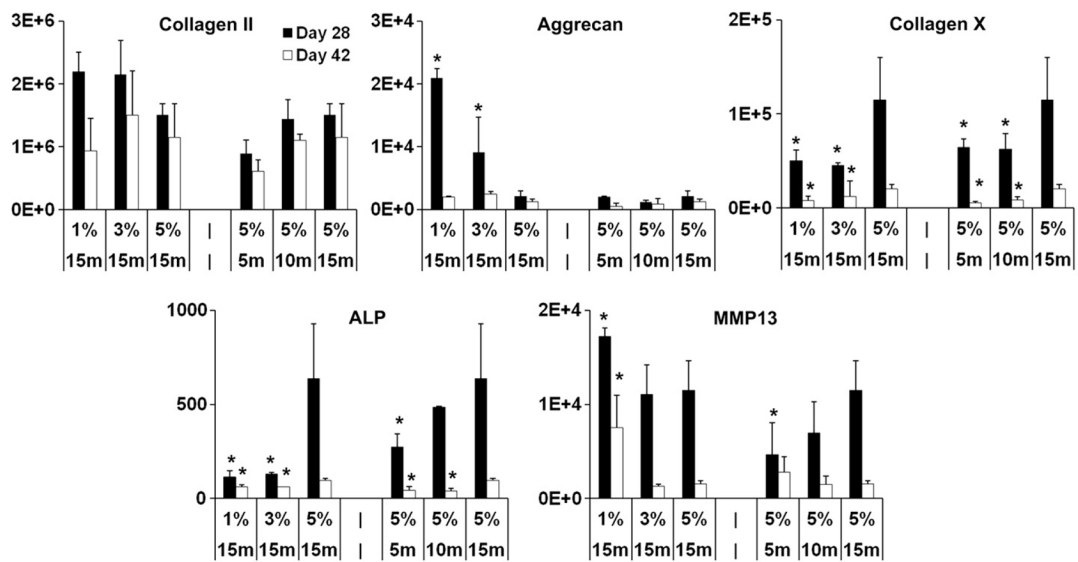


**Fig. 3.** Gene expression (fold change, normalized to GAPDH and to monolayer cells prior to encapsulation) of selected chondrogenic and hypertrophic markers in MSC-laden HA hydrogel constructs after 28 or 42 days of *in vitro* culture. \* $p < 0.05$  vs. 5% 15 min group at the same culture time; ( $n = 4$ ).

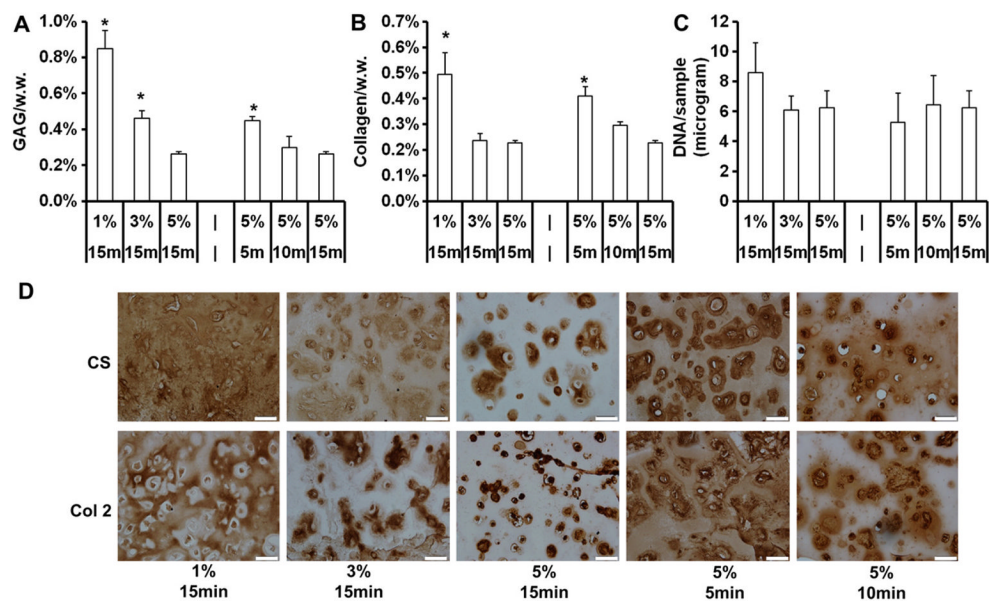


**Fig. 4.** GAG and total collagen content normalized by sample wet weight (A, B) and DNA content per sample (C) of MSC-laden HA hydrogel constructs after 42 days of *in vitro* culture. Immunohistochemical staining for chondroitin sulfate (CS) and type II collagen (Col 2) of MSC-laden HA hydrogel constructs after 42 days of *in vitro* culture (D), scale bar = 50 μm. \* $p < 0.05$  vs. 5% 15 min group at the same culture time; ( $n = 4$ ).

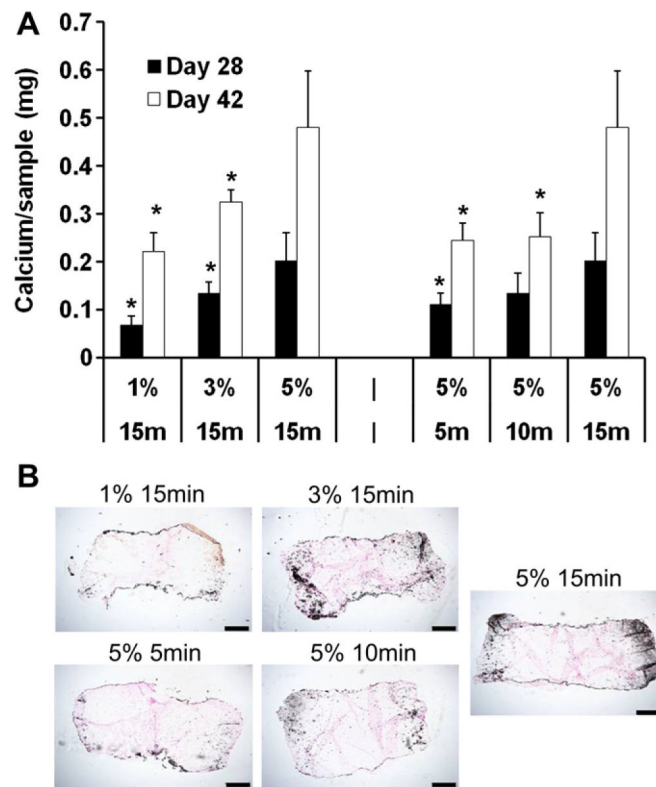


**Fig. 5.** Calcium content of MSC-seeded HA hydrogel constructs after 28 or 42 days of *in vitro* culture (A). Von Kossa staining of HA hydrogel constructs after 42 days of *in vitro* culture (B), bar = 500  $\mu$ m. \* $p$  < 0.05 vs. 5% 15 min group at the same culture time; ( $n$  = 4).

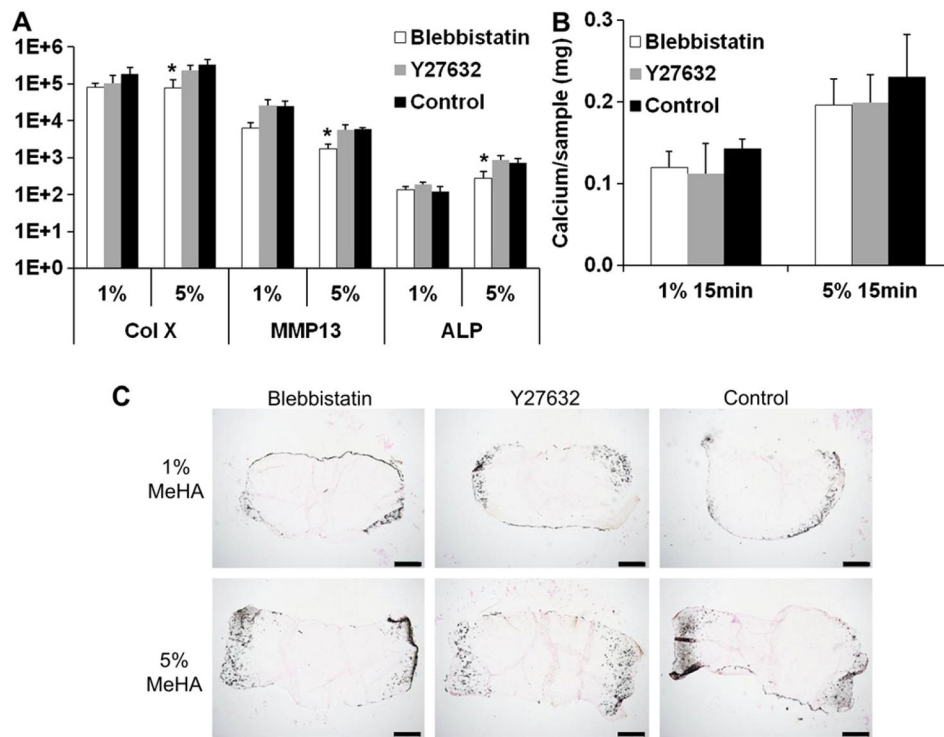


**Fig. 6.** Gene expression (fold change) of selected hypertrophic markers in MSC-laden HA hydrogel constructs (1% or 5% MeHA with 15 min of UV exposure were selected due to the biggest differences observed in the *in vitro* study) after 28 days of *in vitro* culture in the presence of either blebbistatin (10  $\mu$ M) or Y27632 (50  $\mu$ M) or without drugs (Control) (A). Calcium content of the 1% and 5% (w/v) constructs on day 28 (B). Von Kossa staining of constructs on day 28 (C), bar = 500  $\mu$ m. \* $p$  < 0.05 vs. 5% 15 min group at the same culture time; ( $n$  = 4).



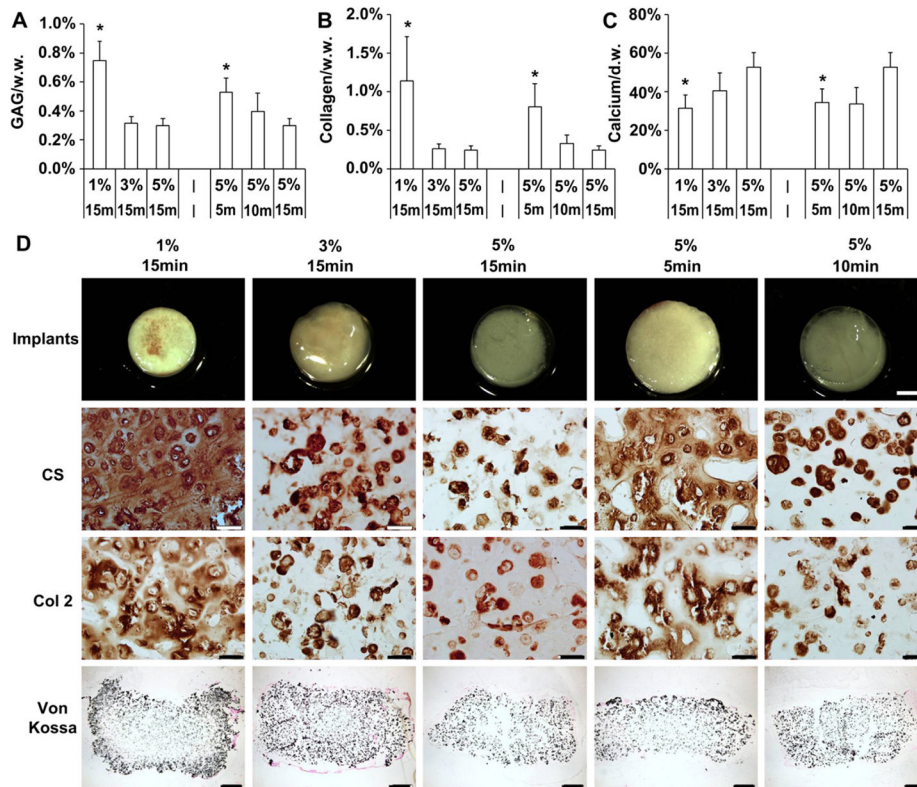


**Fig. 7.** GAG and total collagen content normalized by sample wet weight (A, B) and calcium content normalized by sample dry weight (C) of MSC-laden HA hydrogel constructs after 14 days of *in vitro* culture followed by 28 days of subcutaneous implantation in nude mice (42 days in total). Images of the harvested MSC-laden HA hydrogel implants (scale bar = 2 mm), immunohistochemical staining for chondroitin sulfate (CS) and type II collagen (Col 2) (scale bar = 50  $\mu$ m) and Von Kossa staining of MSC-laden HA hydrogel constructs on day 42 (scale bar = 500  $\mu$ m) (D). \* $p < 0.05$  vs. 5% 15 min group at the same culture time; ( $n = 4$ ).

**Table 1**

Sequences of primers and probes used for real-time PCR. Sequences related to gene type X collagen, alkaline phosphatase, and MMP13 are proprietary to applied Bio-systems Inc. and not disclosed.

<b>Gene</b>	<b>Forward primer</b>	<b>Reverse primer</b>	<b>Probe</b>
GAPDH	AGGGCTGCTTTTA	GAATTTGCCATG	CCTCAACTACAT
	ACTCTGGTAAA	GGTGAAT	GGTTTAC
COL I	AGGACAAGAGGCA	GGACATCAGGCG	TTCCAGTTCGAG
	TGTCTGGTT	CAGGAA	TATGGC
COL II	GGCAATAGCAGGT	CGATAACAGTCTT	CTGCACGAAAC
	TCACGTACA	GCCCCACTT	ATAC
Aggrecan	TCGAGGACAGCGA	TCGAGGGTGTAGC	ATGGAACACGATG
	GGCC	GTGTAGAGA	CCTTTCACCACGA